

# Pseudo-time marching schemes for inverse problems in structural health assessment and medical imaging

H. M. Varma<sup>1</sup>, B. Banerjee<sup>2</sup>, A. K. Nandakumaran<sup>3</sup>, R. M. Vasu<sup>1,\*</sup> and D. Roy<sup>2</sup>

<sup>1</sup>Department of Instrumentation, <sup>2</sup>Department of Civil Engineering, and

<sup>3</sup>Department of Mathematics, Indian Institute of Science, Bangalore 560 012, India

**We propose a self-regularized pseudo-time marching strategy for ill-posed, nonlinear inverse problems involving recovery of system parameters given partial and noisy measurements of system response. While various regularized Newton methods are popularly employed to solve these problems, resulting solutions are known to sensitively depend upon the noise intensity in the data and on regularization parameters, an optimal choice for which remains a tricky issue. Through limited numerical experiments on a couple of parameter re-construction problems, one involving the identification of a truss bridge and the other related to imaging soft-tissue organs for early detection of cancer, we demonstrate the superior features of the pseudo-time marching schemes.**

**Keywords:** Health assessment, medical imaging, Newton algorithm, pseudo-time marching schemes.

## Introduction

RECOVERY of parameter distributions from a set of noisy measurements, often over a small subset of the domain of interest is the main concern in the area of research dealing with the so-called inverse problems. It is usually the case that the solution of a partial differential equation (PDE), referred to as the forward problem, connects the parameters in question to the (partial) measurements of some response variables. Following a discretization of the forward problem, the inverse problem of current interest is one of solving for the discretized parameter vector  $\mu$  through an inversion of the discretized (and possibly nonlinear) system  $u = F(\mu)$ , where  $u$  denotes partial and noisy data and  $F$  a bounded operator (derivable through the discretized forward operator). Given that the Fréchet derivative of  $F$  is ill-conditioned, a ‘weak’ solution is sought, which minimizes  $\|u - F(\mu)\|^2$ . Oftentimes, variants of the Newton algorithm are used to arrive at a local minimum. In order to render the ill-posed parameter recovery problem tractable, a regularization term is added to the mean-square error which has the effect of making

the generalized inverse of Fréchet derivative of  $F$  continuous. An optimal choice of the regularization operator (and the associated regularization parameter) is very important so that the Newton iteration leads to meaningful and smooth solutions to the inverse problem. A number of approaches have been proposed to choose an appropriate regularization operator<sup>1</sup>. The experience has been that none of the approaches work quite satisfactorily, even though all are computationally quite expensive<sup>2</sup>. Another limitation of the standard deterministic approach is its inability to accommodate measurement error as white noise, within the finite dimensional Hilbert space setting used to describe the problem.

In order to overcome some of the limitations of the usual Newton iteration, a stochastic filtering approach, which provides a rigorous probabilistic framework to solve inverse problems has been adopted in the past. For a dynamically evolving state, a stochastic filter provides the route to compute the conditional probability density function (PDF) of the model parameters, given the observation up to the current instant, from which an estimate of the parameter distribution can be had. Examples include the Kalman filter for linear inverse problems or its sub-optimal extensions such as the extended Kalman filter (EKF) and ensemble Kalman filter (EnKF) for nonlinear inverse problems and the posse of optimal particle filters. A catch in the filtering approach is the need of a dynamical model for the evolution of the state, which precludes a number of important applications wherein the measurements are static and the system does not naturally have place for the time variable to benefit from a filtering approach for reconstruction.

One way out of this difficulty, which would bring static problems under the ambit of stochastic filtering is to introduce a pseudo-time under which the parameter is modelled to evolve. This has led to the development of pseudo-dynamic EKF and EnKF (PD-EKF and PD-EnKF respectively) to solve, for example, the elasticity imaging problem from static displacement measurements<sup>3</sup>. The basic idea is to consider  $\mu(t)$ , evolving over pseudo-time, as the solution of a Cauchy problem  $\dot{\mu}(t) = F(\mu(t)) - u(t)$  with  $\mu(0) = \mu_0$  and  $t > 0$  and reconstruct  $\mu$  as a finite-time solution of the above. The PD strategy thus opens up

\*For correspondence. (e-mail: vasu@isu.iisc.ernet.in)

a more general approach to solve the inverse problem leading to various time-recursive methods, including those which use stochastic filtering. For example, a direct time integration, explicit or implicit, of the ordinary differential equation (ODE) leads to self-regularized solutions of the original system of algebraic equations without the need for an inversion of the system matrix. The PD approach, using both stochastic filtering and explicit time integration, has been applied in the recent past to solve inverse problems connected with elastography and diffuse optical tomography<sup>4,5</sup>. It has been observed that the PD algorithm results in robust and self-regularizing procedures leading to recovery of parameter distributions from noisy measurements. When noise is large, typically more than 3%, the PD algorithm is able to reconstruct the parameter distribution with quantitative accuracy, whereas the usual Gauss–Newton method fails.

The aim of the present work is to prove the general applicability and advantages of the PD time marching strategy by solving typical inverse problems in two diverse application areas, structural health assessment involving bridge structures under purely static observations of displacements and medical imaging which aims to recover mechanical property distribution of soft tissue organs from light autocorrelation measurements. These problems are presently tackled by explicit Euler integration of the associated normal equation of the Newton iteration. It is observed through limited comparison with the regularized Gauss–Newton approach that the present approach is less sensitive to measurement noise and performs robustly over a large range of time steps of integration.

### Inversions through pseudo-time marching schemes

In this section, we briefly describe the pseudo-dynamical form of the linearized Gauss–Newton equation for self-regularized recursion over finite time in the reconstruction procedure. For more details, we refer to (ref. 3). Consider the problem of reconstructing the parameter vector  $\mu \in V_\mu \subset \mathbb{R}^n$ , which denotes the finite-dimensional (nodal) discretization of associated scalar field  $\mu(x)$  via finite element shape functions with  $x \in \mathbb{R}^q$  denoting the spatial variable. A similar discretization of the response function  $\mathbf{u}(\mu(x))$  (probably governed by partial differential equations or PDEs) yields the nodal vector  $\mathbf{U} \in V_U \subset \mathbb{R}^d$ . Assuming, without loss of generality, that the elements of the (noisy) measurement vector  $\mathbf{u}^m \in \mathbb{R}^m$  correspond to certain nodal locations, we define  $u \in V_u$  to be the subset of  $\mathbf{U}$  corresponding to  $\mathbf{u}^m$ ;  $m \leq d$ . For most applications, we have  $m \ll d$  resulting in very large null spaces and the associated numerical difficulties including multiplicity of solutions. A common regularization technique is to penalize the optimization functional with some extra terms, broadly known as Tikhonov regularization, leading to the following optimization problem.

$$\min_{\mu \in \mathbb{R}^n} \sum_{i=1}^S \frac{1}{2} \|\mathbf{u}_i(\mu) - \mathbf{u}_i^m\|^2 + \frac{\lambda}{2} \|L(\mu)\|^2, \quad (1)$$

where  $u(\mu)$  is computed using

$$K(\mu)\mathbf{U} = \mathbf{f}. \quad (2)$$

Here  $L$  denotes the penalization operator on  $\mu$ ,  $\lambda$  the regularization parameter,  $\|\cdot\|$  the  $L_2$  norm and  $S$  is the number of load (source) cases. Moreover,  $K$  denotes the parameter dependent system (stiffness) matrix and  $\mathbf{f}$  the non-parametric source (force) vector. Subscript ‘ $i$ ’ refers to the response corresponding to the  $i$ th source case. The essential optimality condition (normal equation) for the problem is

$$g(\mu) = \sum_{i=1}^S J_i(\mu)^T (\mathbf{u}_i(\mu) - \mathbf{u}_i^m) + \lambda L'(\mu) = 0, \quad (3)$$

where  $J_i(\mu) = (\partial \mathbf{u}_i(\mu) / \partial \mu)$  is the Jacobian matrix and  $L'(\mu) = (\partial L(\mu) / \partial \mu)$ . The above nonlinear equation is generally solved using successive linearizations with the Hessian approximated as  $H = \sum_{i=1}^S J_i^T(\mu) J_i(\mu)$  (Gauss–Newton approximation). This leads to the following linear equation in the increment  $\Delta\mu$ .

$$(H + \lambda L''(\mu))\Delta\mu + G(\mu) = 0 \quad (4)$$

with  $\mu$  being the linearization point and  $G$  to be defined here. Note that the addition of a regularization term in the optimization functional leads to a different minimization problem from the one originally envisaged. The closeness of solutions of the regularized and original problems is greatly influenced by the penalization terms and, in particular, by the parameter  $\lambda$ . The operator  $L''$  is helpful in tackling the numerical difficulties owing to the null space of the linearized operator. Moreover, it should be so chosen as to account for any available *a priori* knowledge on spatial distributions of the parameters to be recovered. While an appropriate choice of regularization terms could lead to useful solutions, small variations in these terms could as well lead to severe degradation of solutions.

One way of obtaining an iterative solution to a nonlinear inverse problem, as above, whilst avoiding an explicit inversion of the linearized operator would be to introduce artificial dynamics and consider the solution to be the response of the artificially evolving dynamical system after some finite time (before the solution diverges). This may be thought of as a special case of continuation or homotopy-based approaches. For instance, the solution of a system of algebraic equations (with positive semi-definite coefficient matrix following linearization) may be thought of as the steady-state solution of a system of ODEs. In this context, ‘time’ is a pseudo-variable and re-

cursor over a chosen step size through numerical integration plays the role of iterations. Moreover, this artificial dynamics may evolve on an invariant manifold (a Lie manifold) and thus enable development of robust numerical schemes that may not diverge. It is of interest to note that Landweber iterations, which correspond to an explicit Euler time discretization of a system of ODEs describing the artificial dynamics of an inverse problem<sup>2,6</sup>, have a self-regularized character depending upon the time-step. Keeping these in mind we form a pseudo-dynamical counterpart of the Gauss–Newton iterative update equation. In particular, by adding a fictitious time derivative term in eq. (4) with  $\lambda = 0$ , we obtain the linearized ODE in  $(t, t + \Delta t]$ .

$$\dot{\mu} + H(\mu^*)(\mu(t) - \mu^*) + G(\mu^*) = 0, \tag{5}$$

where  $G(\mu^*) := \sum_{i=1}^S J^i(\mu^*)^T (\mathbf{u}_i(\mu^*) - \mathbf{u}_i^m)$ . The over-dot represents the time derivative and  $\mu^*$  is the linearization point in the  $n$ -dimensional vector space  $V_\mu$ . Note that we have removed the regularization term while forming the dynamical system and that the ODE contains  $\mathbf{u}^m$ , which is noisy. Upon integration over indefinite time intervals, solutions may diverge. In order to avoid such blow-off of solutions, we intend to use a stopping criterion and thus integrate only over a finite time interval. The stopping criterion may be arrived at through the discrepancy principle or any other suitable scheme depending upon the user requirement.

The solution of the linearized ODE (5) may be written as

$$\begin{aligned} \mu(t + \Delta t) = & \exp([-H(\mu^*)](\Delta t))\mu(t) \\ & + \int_t^{t+\Delta t} \exp([-H(\mu^*)](t + \Delta t - s))\mathbf{f} \, ds, \end{aligned} \tag{6}$$

where  $\mathbf{f} = H(\mu^*)\mu^* - G(\mu^*)$  is a constant forcing. Following the concept of local linearization, the linearization point  $t^*$  (such that  $\mu^* := \mu(t^*)$ ) could be chosen anywhere in the closed interval  $[t, t + \Delta t]$  without affecting the formal error order. While choosing  $t^* = t$  yields the explicit phase space linearization (PSL)<sup>7</sup>,  $t^* = t + \Delta t$  results in the implicit locally transversal linearization (LTL)<sup>8</sup>. Denoting  $h = t_{k+1} - t_k$  to be the time step and  $\mu_k := \mu(t_k)$ , the explicit PSL map corresponding to the continuous update eq. (6) is written as

$$\begin{aligned} \mu_{k+1} = & \exp([-H(\mu_k)](t_{k+1} - t_k))\mu_k \\ & + \int_{t_k}^{t_{k+1}} \exp([-H(\mu_k)](t_{k+1} - s))\mathbf{f}_k \, ds \end{aligned} \tag{7}$$

with

$$\mathbf{f}_k = H(\mu_k)\mu_k - G(\mu_k). \tag{8}$$

We thus bypass computing the inverse of the Hessian ( $J^T J$ ) or its modifications, used with the regularization terms. The fact that exponentiation is being used whilst obtaining the time stepping algorithm should enable a geometrically consistent progression on the associated (nonlinear) Lie manifold and thus provide a ‘natural’ stabilization for the inverse problem at hand. In this sense, a connection with the Tikhonov type approach could also be brought out. While a detailed theoretical exploration of such issues is outside the present scope, the following argument, proposed in ref. 9 and adapted for the present case, provides useful insight. Consider the singular value decomposition of the Jacobian  $J(\mu_k) := J_k = U_k[\text{diag}(\omega_i)] \times V_k^T$ , valid over  $t \in (t_k, t_{k+1}]$ . Then, the explicitly linearized solution, given by eq. (7), may be recast as

$$\begin{aligned} \mu_{k+1} = & V_k \text{diag}\{(1 - e^{-h\omega_i^2})\} U_k^T \mu_k \\ & + V_k \text{diag}\left\{(1 - e^{-h\omega_i^2}) \frac{1}{\omega_i}\right\} U_k^T \mathbf{f}_k. \end{aligned} \tag{9}$$

Thus, the effect of recursion with a step size  $h$  is to appropriately modify (regularize) the terms containing the inverse  $\omega_i^{-1}$  of the singular values  $\omega_i$ , especially near the lower end of the spectrum. Hence, while the terms containing small  $\omega_i$ ’s get damped over finite recursions, the ones containing larger  $\omega_i$ ’s remain nearly unaffected.

From the numerical standpoint, the computation of matrix exponentials is the key cost that might limit the viability of the method for higher dimensional problems. In such cases, one may exploit the sparse structure of  $J$  along with a Krylov subspace projection to speed up computations<sup>10</sup>. Both the Gauss–Newton method (that requires matrix inversion and hence  $O(n^3)$  operations) and the pseudo-dynamical strategy (that employs matrix exponentiation, again involving  $O(n^3)$  operations)<sup>11</sup> have similar computational overheads over a single iteration. Thus a possible difference in the cost of computation should depend on the number of iterations needed for convergence, given a tolerance, in each method. Our limited numerical exploration suggests that the pseudo-dynamical approach typically needs marginally higher number of iterations vis-à-vis its Gauss–Newton counterpart. However an adaptive strategy for choosing the time step in the pseudo-dynamical approach could reduce the number of iterations, making it as efficient as the Gauss–Newton method.

### Applications

To illustrate the universal applicability of the pseudo-time marching schemes, we take a couple of nonlinear inverse problems that are typically encountered in two diverse disciplines, viz. structural system identification and non-invasive mechanical property assessment in soft-tissue organs.

System identification of bridges

Before presenting the numerical results, a word about the stopping rule for the time marching schemes. Due to the unbounded nature of the operator governing the inverse problem, an improper stopping criterion may lead to blow-offs. We define the measure of misfit as

$$M = \sum_{i=1}^S \frac{\|\mathbf{u}^i - \mathbf{z}^i\|}{\|\mathbf{z}^i\|} \quad (10)$$

$\mathbf{U} \in \mathbb{R}^m$  is the computed response and  $\mathbf{z} \in \mathbb{R}^m$  the statically measured response. We stop iterations when  $\mathbf{M}$  goes below a specified tolerance.

We choose a multi-span truss as taken in ref. 12. The structure is modelled via linear truss element with transverse and axial displacement degrees of freedom per node. A four-span bridge with 105 truss elements and 44 nodes subjected to static loading is considered. The  $c/s$  area selected for each truss element is 2500 mm<sup>2</sup> and the Young's modulus of the material is 200 GPa. Five damaged elements localized in the first left bay are introduced in the structure (Figure 1 *b*). The skeletal structure model is adopted with element-wise constant material property distributions. Denoting  $\alpha$  as the damage index vector, the discrete forward problem is:

$$K(\alpha)\mathbf{U} = \mathbf{f}. \quad (11)$$

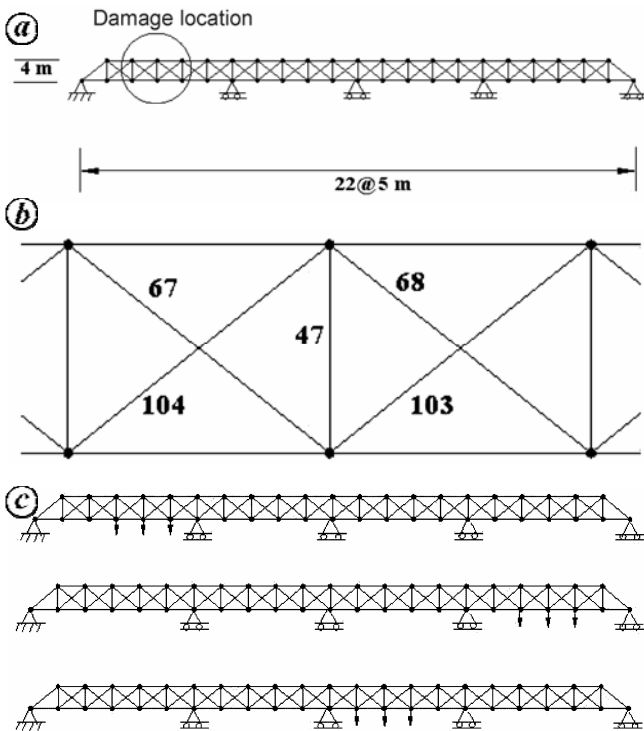


Figure 1. *a*, Multi-span truss structure and damaged members. *b*, Enlarged view of the damaged members. *c*, Three different loading cases considered.

The element damage index ( $\alpha_e$ ) is defined as  $K_{\text{damaged}}^e = (1 - \alpha_e) K_{\text{undamaged}}^e$ ,  $0 \leq \alpha_e \leq 1$ , with 'e' referring to the  $e$ th element. The goal is to determine the discontinuous damage index profile with a partial measurement of the deformation quantities. We now intend to validate the proposed schemes without taking recourse to any experimentally procured data. For generating the simulated measurements, one way is to solve the discretized forward problem and then additively perturb the targeted ('measured') displacement components at the measurement nodes with noise, generated as a set of independent and identically distributed (IID) random variables of a specified intensity. Presently, we assume that the set of measurements contains only the transversal displacement components at a few nodes. Identification of the isolated damage locations and magnitudes typically needs measurements corresponding to multiple load cases. We con-

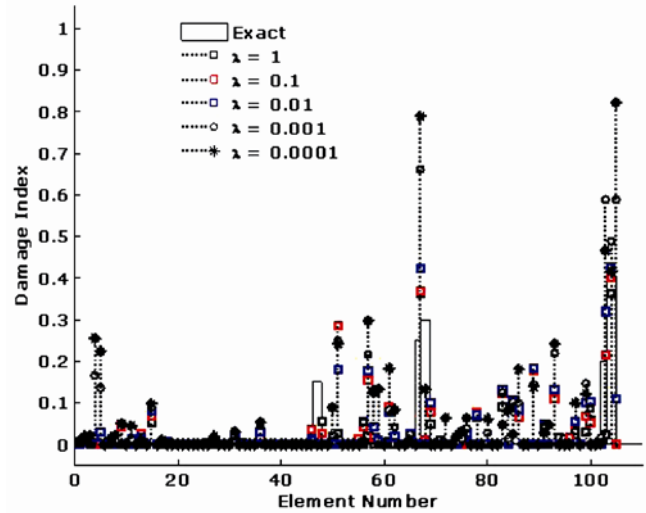


Figure 2. Results via the GN method with 1% measurement noise.

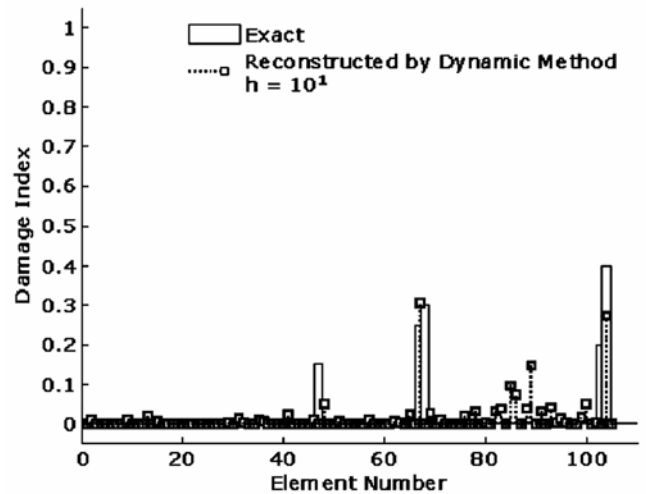


Figure 3. Results via the pseudo-dynamic method with 1% measurement noise.

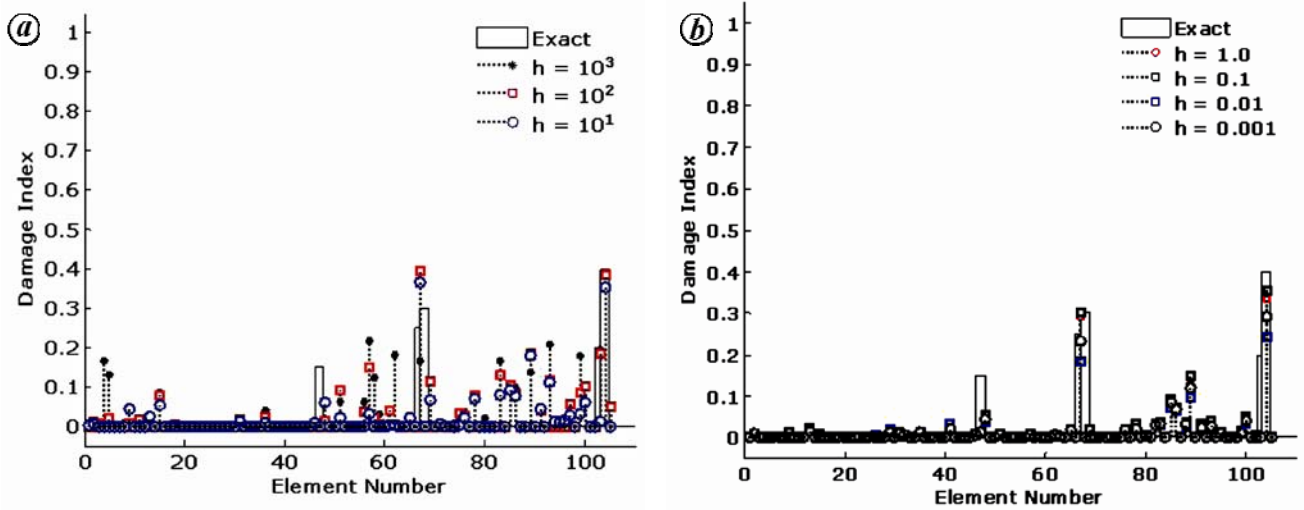


Figure 4. Sensitivity with time step for pseudo-dynamic method for 1% measurement noise. *a*, Time step  $\geq 10$ . *b*, Time step  $\leq 1$ .

consider three specific load cases as shown in Figure 1 *c*. We first use the conventional regularized Gauss–Newton method (GNM) to bring out the sensitivity of reconstructions to the regularization parameter. Results via the GNM for different regularization parameters are shown in Figure 2. It is observed that the best regularization parameter is 0.01. Nevertheless, as shown in Figure 2, a small variation about this optimal value drastically affects the reconstruction. Results via the deterministic time-marching approach, shown in Figure 3, demonstrate that the damage profile is well reproduced and quantified. Sensitivity of the reconstruction to time steps is shown in Figure 4. We observe that, even with a very high step size (e.g.  $10^3$ ), the algorithm is able to correctly identify the damage zones in the structure.

*Recovery of particle diffusion coefficient from light intensity autocorrelation*

Here we consider the propagation of coherent light, through a tissue-like object, whose amplitude autocorrelation is affected by properties both the optical (for example, absorption and scattering coefficients) and mechanical (for example, the mean-square displacement, MSD, of particles undergoing temperature-induced Brownian motion, which in a linear visco-elastic medium is assumed to have a linear time dependence  $6D_B\tau$ ,  $D_B$  being the particle diffusion coefficient). The propagation of the un-normalized field autocorrelation  $G(r, \tau)$  is governed by the PDE

$$\nabla \cdot \kappa(r) \nabla G(r, \tau) - (\mu_a + 2k_0^2 \mu'_s D_B \tau) G(r, \tau) = -q_0(r - r_0) \tag{12}$$

for  $r \in \Omega$ , with the boundary condition,

$$\kappa(m) \frac{\partial G(m, \tau)}{\partial \hat{n}} + G(m, \tau) = 0, \tag{13}$$

where  $m \in \partial\Omega$ . Here  $k_0$  is the modulus of the propagation vector of light,  $\mu_a$  and  $\mu'_s$  are respectively the absorption and reduced scattering coefficients of the object,  $\kappa(r)$  is the optical diffusion coefficient and  $q_0(r - r_0)$  is the point source at  $r_0$ . We intend to recover  $D_B$  from a set of boundary measurements of a quantity related to  $G(r, \tau)$ , which is the intensity autocorrelation

$$g_2(m, \tau) = 1 + \left| \frac{G(m, \tau)}{G(m, 0)} \right|^2.$$

For this, we discretize eqs (12) and (13) using FEM and obtain a set of algebraic equations  $K(D_B)\mathbf{G} = \mathbf{q}$ . The deterministic method seeking the minimization of an error functional, as explained in the previous section, leads to Levenberg–Marquardt (LM) update equation (a variation of the GNM).

$$(\Delta D_B)_{i+1} = [J^T((D_B)_i)J((D_B)_i) + \lambda_{i+1}I]^{-1} \times J^T(D_B)_i(g_2^{(m)} - g_2((D_B)_i)). \tag{14}$$

Here  $g_2^{(m)}$  is the experimentally measured intensity autocorrelation (on the boundary nodes) and  $g_2((D_B)_i)$  is its computed counterpart for the current  $D_B$ .

The Jacobian  $J(D_B)$  has to be evaluated for the measurement  $g_2(m, \tau)$ , which is obtained from  $G(m, \tau)$  using the measurement operator  $\mathbf{M}$ :

$$\mathbf{M}(G(m, \tau)) = 1 + \left| \frac{G(m, \tau)}{G(m, 0)} \right|^2. \tag{15}$$

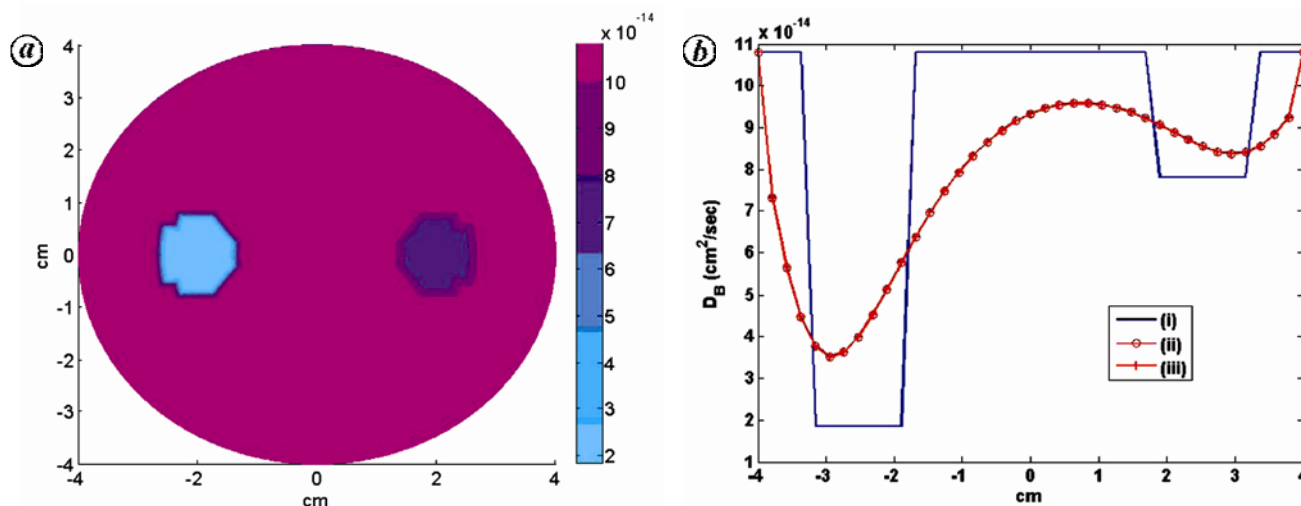


**Figure 5.** *a.* Reference profile. *b.* Comparison of original cross-sectional profile (i) with those reconstructed via LM method (ii) and pseudo-time marching scheme (iii) from data with 1% noise.

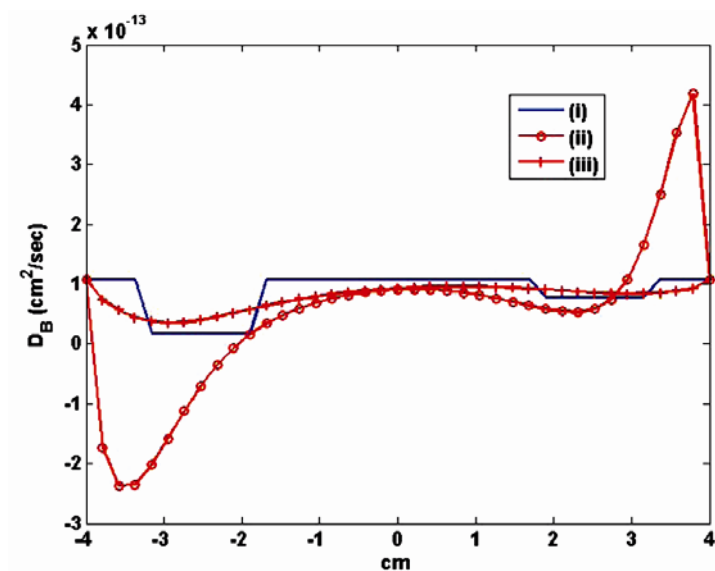


**Figure 6.** Cross-sectional profiles, reconstructed via (ii) LM algorithm and (iii) pseudo-time marching scheme, from data with 2% noise compared with the original profile (i).

For quick computation of the Jacobian, the adjoint method that makes use of the reciprocity relation of light propagation is made use of. For details, we refer to ref. 13.

The LM algorithm is used to recover  $D_B$  from simulated intensity autocorrelation data. The circular object used in the simulation is of 8 cm diameter with the following optical and mechanical properties:  $\mu_a^b = 0.001 \text{ cm}^{-1}$ ,  $\mu_s^b = 8 \text{ cm}^{-1}$  and  $D_B^b = 0.0 \text{ cm}^2/\text{s}$ . The object has two circular inhomogeneous inclusions in  $D_B$ , one at  $(-2.5 \text{ cm}, 0 \text{ cm})$  of  $D_B^b = 0.1 \times 10^{-8} \text{ cm}^2/\text{s}$  and the other at  $(2.5 \text{ cm}, 0 \text{ cm})$  of  $D_B^b = 0.4 \times 10^{-8} \text{ cm}^2/\text{s}$ . The experimental data set is generated by solving the forward equa-

tion for  $G(r, \tau)$  using a finer mesh than used in the inversion and corrupting the solution with Gaussian noise.

The reconstruction using the pseudo-time marching method, based on data with 1% noise, is shown in Figure 5b. For this case, the LM algorithm also produces nearly identical reconstruction. When noise is increased to 2%, the LM algorithm fails to appropriately recover the  $D_B$  field whereas the pseudo-time marching method works quite satisfactorily. This is shown in the cross-sectional profiles of Figure 6, where (i) is for the reference  $D_B$  field, and (ii) and (iii) are obtained from the LM and the pseudo-time marching methods respectively. It is observed that the quantitative accuracy and the contrast recov-

ery, as obtained through the pseudo-dynamic approach, are distinctively superior vis-a-vis the LM algorithm, especially for 2% and still higher data noise levels.

### Concluding remarks

We have shown through limited numerical simulations that the proposed pseudo-time marching scheme is self-regularized (in that it does not need an explicit specification of any regularization parameter) and works more robustly in respect of handling data noise in comparison with regularized Gauss–Newton methods, popularly used for nonlinear inverse problems involving reconstruction of system parameters. The two illustrative system identification problems we have discussed, one concerning a bridge structure and the other involving soft tissue organs for medical diagnosis, help bring forth these advantages with the pseudo-dynamic scheme.

- 
1. Vogel, C., *Computational Methods for Inverse Problem*, SIAM, Philadelphia, 2002.
  2. Engl, W. H., Hanke, M. and Neubauer, A., *Regularization of the Inverse Problem*, Kluwer Academic Publishers, 2000.
  3. Banerjee, B., Roy, D. and Vasu, R. M., A pseudo-dynamical systems approach to a class of inverse problems in engineering. *Proc. R. Soc. A*, 2009, **465**, 1561–1579.
  4. Banerjee, B., Roy, D. and Vasu, R. M., A pseudo-dynamic sub-optimal filter for elastography under static loading and measurements. *Phys. Med. Biol.*, 2009, **54**, 285–305.
  5. Yalavarthy, P. K., Roy, D. and Vasu, R. M., A pseudo-dynamical stochastic filter for reconstructing diffuse optical tomographic images. *IEEE Trans. Med. Imaging*, 2009 (under review).
  6. Tautenhahn, U., On the asymptotical regularization of non-linear ill-posed problems. *Inverse Problems*, 1994, **10**, 1405–1418.
  7. Roy, D., Phase space linearization for non-linear oscillators: deterministic and stochastic systems. *J. Sound Vibr.*, 2000, **231**, 307–341.
  8. Roy, D., A numeric-analytic technique for nonlinear deterministic and stochastic dynamical systems. *Proc. R. Soc. A*, 2001, **457**, 539–566.
  9. Ascher, U., Huang, H. and Doel, K. van den, Artificial time integration. *BIT*, 2007, **47**, 3–25.
  10. Saad, Y., Krylov subspace methods on supercomputers. *SIAM J. Sci. Stat. Comput.*, 1989, **6**, 1200–1232.
  11. Moler, C. and Van Loan, C., Nineteen dubious ways to compute the exponential of a matrix, twenty-five years later. *SIAM Rev.*, 2003, **45**, 1–46.
  12. Kouchmeshky, B., Aquino, W., Bongard, J. C. and Lipson, H., Co-evolutionary algorithm for structural damage identification using minimal physical testing. *Int. J. Num. Meth. Eng.*, 2007, **69**, 1085–1107.
  13. Varma, H. M., Vasu, R. M. and Nandakumaran, A. K., Direct reconstruction of complex refractive index distribution from boundary measurement of intensity and normal derivative of intensity. *J. Opt. Soc. Am. A*, 2007, **24**, 3089–3099.
-